

**Ferroan Anorthosite 60025: Magma Ocean Product – and more!** Torcivia M.A.<sup>1</sup> and Neal C.R.<sup>1</sup> <sup>1</sup>Dept. Civil & Env. Eng. & Earth Sciences, University of Notre Dame, Notre Dame IN, 46556; mtorcivi@nd.edu

**Introduction:** The Ferroan Anorthosite (FAN) group of lunar samples is thought to represent the earliest example of the primordial lunar crust [1], according to Lunar Magma Ocean (LMO) theory [2]. Recent radiogenic isotope studies on a suite of FANs (e.g., [3,4]) have challenged the validity of LMO theory based on the large range of radiometric ages for FANs (~268 m.y.). However, it is possible that the introduction of an insulated lid coupled with tidal heating could account for a more extended LMO crystallization and explain the range of ages for FANs [5]. Assuming all FANs crystallized from the LMO, calculated equilibrium liquids from mineral trace elements can be compared with various LMO modeling efforts (e.g., [5-9]). Initial results using this approach have been encouraging [10]. Equilibrium liquids that have lower incompatible trace element (ITE) abundances would have crystallized from the LMO earlier than those with higher ITE abundances [11]. Ideally, this relative sequence should match the range of FAN radiometric ages. This study uses a combination of electron microprobe (EMP) and LA-ICP-MS analysis to calculate parent melt plagioclase compositions and compares them to models described by Neal and Draper [10,11].

**Methods:** The main sample of focus was lunar sample 60025, which has been described as ‘pristine’ [5]. The initial step was to obtain petrographic photomosaics of a suite of FANs that have published radiometric age dates [2], focusing on lunar sample 60025 (daughter samples 21, 134, 269, and 273; Fig. 1). All thin sections show 60025 as severely brecciated. Each section was analyzed by electron microprobe (EMP) at the University of Notre Dame using a Cameca SX-50 to determine major & minor element abundances in both plagioclase and assorted mafic grains. EMP spots were taken as core-rim pairs in all plagioclase grains. Sample 60025,273 was then analyzed for trace element concentration using laser ablation (LA) ICP-MS. Partition coefficients for the plagioclase grains were calculated using the method developed by [12].

**Results: Electron Microprobe:** Anorthite ( $An$ ) content vs. FeO (wt. %) for cores and rims is shown in Fig. 2. The cores of the plagioclase grains show evidence of a fractionation trend. As  $An$  decreases, FeO increases (consistent with a magma evolving through crystallization), although there are only a few points with  $An > 98$ . The majority of core and rim data fall within  $An_{97-98}$  suggesting that most crystals are

equilibrated. Is this from the primary LMO cumulate origin or a subsequent impact event?

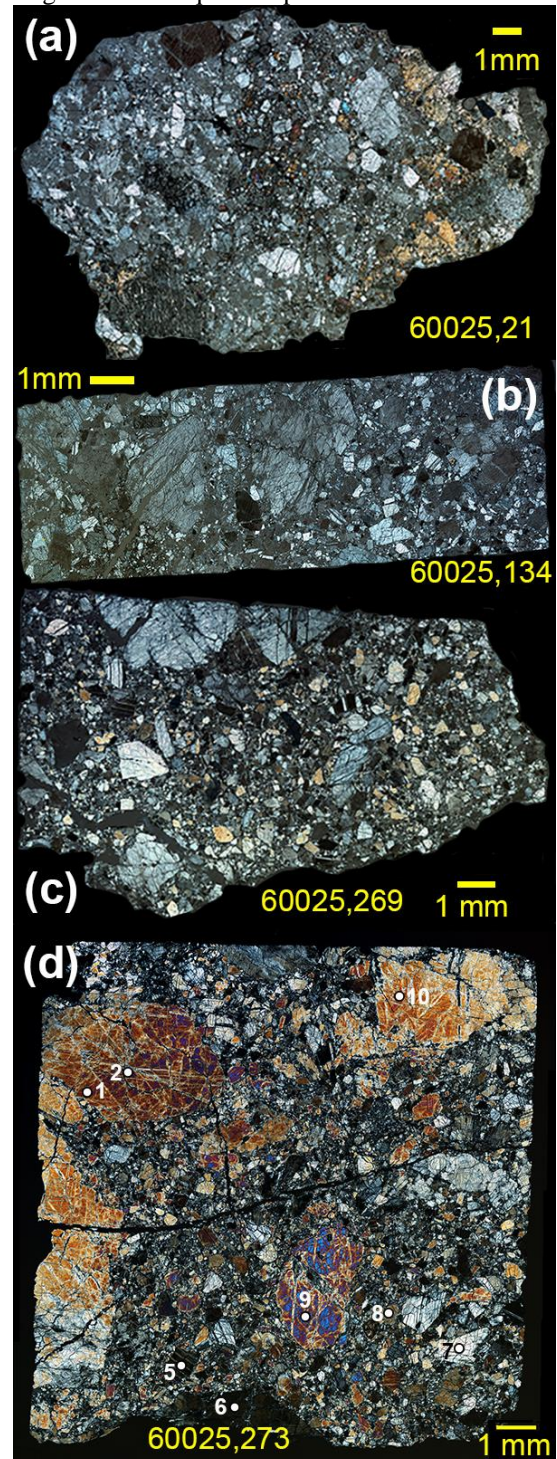


**Figure 1:** XPL views of four 60025 thin sections: (a) ,21; (b) ,134; (c) ,269; (d) ,273 with laser spots.

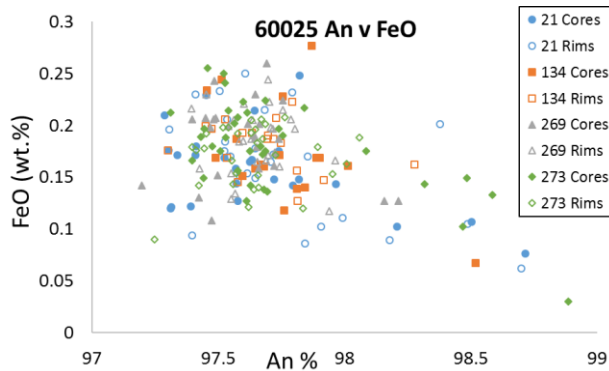


**Figure 2:** Electron microprobe data of percent anorthite (An) and FeO (wt.%) from cores and rims of plagioclase grains in 4 daughter samples of 60025.

*Laser Ablation ICP-MS:* Figure 3a depicts REE profiles from plagioclase crystals from 60025, 273.

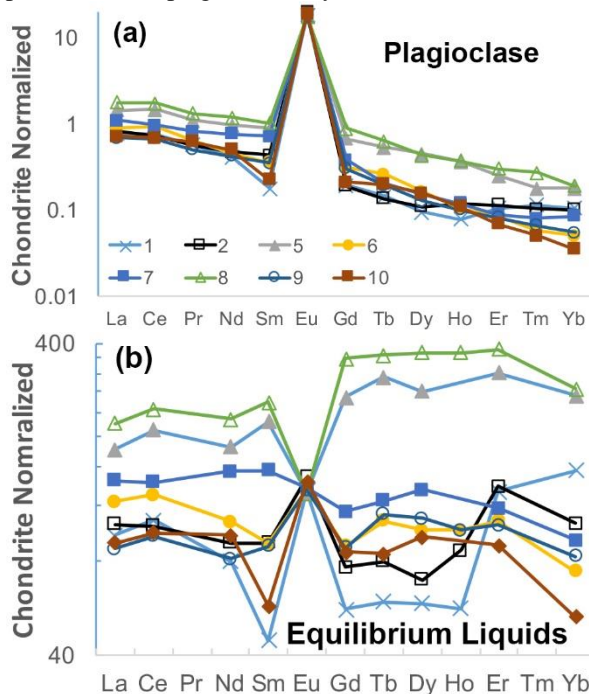


**Figure 3:** Chondrite normalized [13] REE Profiles for Plagioclase (a) and calculated equilibrium liquids (b) using the method described in [12],  $T = 1273\text{K}$ .

Analyses 1, 2, 9, and 10 are from the cores of the largest grains in 60025,273 (Fig. 1d). These should represent the earliest crystallized plagioclase of the FAN cumulate. These plagioclase analyses contain the lowest REE contents (Fig. 3a). The Plagioclase REE profiles 5, 6, 7, and 8 are from smaller crystals (Fig. 1d) and have higher light REE abundances. Crystals 5 and 8 also have higher middle and heavy REE. The profiles for points 1 and 10 show a unique downturn at Sm (Fig. 3a).

**Discussion:** Equilibrium liquids can be calculated using the method refined in [12]. Equilibrium liquids calculated for the plagioclase data show that data at Er-Yb for analyses 1 and 2 probably reflect contamination from pyroxene (the HREE data for 1 and 2 flatten out in Fig. 3a). What is shown by this work is that plagioclase compositions from 60025 span a range of compositions, but are these all consistent with derivation from an evolving LMO liquid [14]? Analyses 1, 2, 9, and 10 exhibit slightly LREE enriched equilibrium liquids (Fig. 3b), consistent with LMO crystallization models after ~80% crystallization [14]. However, the liquids all have positive Eu anomalies (as does the equilibrium liquid for analysis 5; Fig. 3b). Analysis 7 has a slightly LREE enriched REE profile with no Eu anomaly. Analyses 5 and 8 yield equilibrium liquids with the highest REE abundances, but exhibit LREE depleted profiles, inconsistent with derivation from an evolving LMO liquid (e.g., [14]) with a strong negative Eu anomaly.

**Ages:** Two distinct radiometric ages have been reported for 60025:  $4.367 \pm 0.011$  Ga [15];  $4.44 \pm 0.02$  Ga [16]. Petrologically, this sample was described as being *probably a mixture of several FAN lithologies* [17]. Using the relative age dating method of [11], age estimates of the two groups of plagioclases can be made on the basis of their equilibrium liquid compositions. Analyses 1, 2, 9, and 10 yield an average age of  $4.516 \pm 0.01$  Ga, which is much older than the two published ages. The remaining analyses yield ages similar to the 4.44 Ga age [16], suggesting that published ages represent mixtures of FAN material, although the younger age from [15] resulted from multiple chronometers (but see [18]). Future studies will repeat this experiment on FAN samples with dates published in [2] specifically looking at samples 67075 and 62236.

**References:** [1] Dowty E. et al. (1974) *EPSL* 24, 15-25. [2] Taylor S.R. & Jakes P. (1974) *PLSC* 5, 1287-1305. [3] Borg L.E. et al. (2011) *Nature* 477, 7072. [4] Gaffney A. & Borg L. (2014) *GCA* 140, 227-240. [5] Elkins-Tanton L.T. et al. (2011) *EPSL* 304, 326-336. [6] Snyder G. et al. (1992) *GCA* 56, 3809-3823. [7] Rapp J. & Draper D. (2012) *LPSC* 43, #2048. [8] Rapp J. & Draper D. (2013) *LPSC* 44, #2732. [9] Rapp J. & Draper D. (2014) *LPSC* 45, #1527. [10] Neal C.R. and Draper D.S. (2016) *LPSC* 47, #1165. [11] Neal C.R. & Draper D.S. (2017) *LPSC* 48. [12] Hui H. et al. (2011) *GCA* 75, 6439-6460. [13] Anders E. & Grevasse N. (1989) *GCA* 53, 197-214. [14] Neal C.R. & Davenport J. (2014) *LPSC* 45, #1181. [15] Borg L.E. et al. (2011) *Nature* 477, 70-72. [16] Carlson R. & Lugmair G. (1988) *EPSL* 90, 119-130. [17] James O. et al. (1991) *PLPSC* 21, 63-87. [18] Torcivia M.A. & Neal C.R. (2017) *LPSC* 48.